

# We are IntechOpen, the world's leading publisher of Open Access books Built by scientists, for scientists

6,900

Open access books available

185,000

International authors and editors

200M

Downloads

Our authors are among the

154

Countries delivered to

TOP 1%

most cited scientists

12.2%

Contributors from top 500 universities



WEB OF SCIENCE™

Selection of our books indexed in the Book Citation Index  
in Web of Science™ Core Collection (BKCI)

Interested in publishing with us?  
Contact [book.department@intechopen.com](mailto:book.department@intechopen.com)

Numbers displayed above are based on latest data collected.  
For more information visit [www.intechopen.com](http://www.intechopen.com)



---

# Effect of Source Impedance on Hybrid Wind and Solar Power System

---

Mu-Kuen Chen and Chao-Yuan Cheng

Additional information is available at the end of the chapter

<http://dx.doi.org/10.5772/54495>

---

## 1. Introduction

Large wind turbines use mechanical systems, such as geared or gearless devices to increase the speed of the generator. In addition, an inverter is employed to adjust the output voltage to exceed the grid value. With its phase leading the bus phase, wind power can be integrated into the grid bus. The integration can be easily realized owing to negligible impedance of the utility bus. The main issues for wind-power generating systems include fluctuations in output voltage and quality of power supplied to the utility power system. In small renewable energy systems, wind power and solar energy are integrated to improve the reliability of the individual power system. Conventionally, the AC output voltage of the wind turbine is rectified, and then combined with the output voltage of the solar cell to charge the battery and provide power supply to the load. To characterize the battery, the Thevenin battery model considering the nonlinear effect of source impedances was proposed. A battery evaluation test system was employed to validate this model. The curve of test results follows entirely the theoretical calculation [1]-[3]. For photovoltaic application, the inner resistance of solar panel was also included in the theoretical analysis. The maximum power point tracking (MPPT) of solar panel for different insolation levels verified the proposed solar cell model. The MPPT technique adjusted continuously the battery-charging rate and obtained shorter charge time [4]. It was reported that a dual battery configuration with deep-cycle batteries can increase the available capacity. Moreover, the system may achieve optimum utilization of the PV array and proper maintenance of the storage battery [5]. In another research, a microcontroller was employed to adjust the maximum charging current according to the PV power production and battery voltage level. Using this method, better exploitation of the power produced by the PV power source can be achieved. Moreover, battery lifetime can be increased by restoring high state of charge (SOC) in short charging time [6]. Another study compared the performance of equal

rate charging, proportional rate and pulse current charging in charging multiple batteries. The total charging time is shortest when using pulse current charging strategy. All the batteries become fully charged almost simultaneously when they are charged with proportional rate or pulse current method [7]. The optimum size of the PV module for a specific wind turbine to meet the load requirement for the hybrid wind/PV system was investigated in order to minimize the overall cost of the system [8] - [9]. Nevertheless, the effect of source impedance in a small hybrid wind/PV system has not yet been investigated. In this study, theoretical analysis shows that it is difficult to obtain both wind power and solar energy at the same time by traditional methods, which is verified by field test. To overcome such problem, a micro-processor-based controller design for detecting instantaneous voltage variations of both energy sources is proposed, and a charge controller is employed to optimize the charging operation.

## 2. Theory and analysis

Owing to the large variation in the wind and solar energy, the converter is employed to provide the stable power for normal application. When only one energy source supplies the load, as shown in Fig.1(a), the voltage and frequency of the converter output is adjusted to meet the load specification. In Fig. 1(b), both wind and solar energy supply the same load simultaneously. In addition to the load requirement, the voltage and frequency of both converter outputs are adjusted such as the two energy sources can supply the load at the same time. In case of the DC-DC converter, only the output voltage of both converters should be adjusted to charge the same load.

In a small hybrid power system, a battery is usually utilized to store the renewable energy to improve the reliability of the system. Moreover, to simplify the power system, the power source charges directly the battery. Figure 2 shows the conventional charging system, in which the rectified DC voltage charges two batteries. In addition to source voltages  $E_w$ ,  $E_1$  and  $E_2$ , charging currents  $I_1$  and  $I_2$  are also determined by source resistances  $r_w$ ,  $r_1$  and  $r_2$  for the wind power and the two batteries, respectively. The output voltage  $V_0$  is the summation of  $V_{0w}$ ,  $V_{01}$  and  $V_{02}$  from wind power and batteries  $E_1$  and  $E_2$ , respectively. According to the circuit theory, the equations for  $V_{0w}$ ,  $V_{01}$  and  $V_{02}$  are as follows:

$$V_{0w} = E_w \left( \frac{r_1 r_2}{r_w r_1 + r_1 r_2 + r_w r_2} \right) \quad (1)$$

$$V_{01} = E_1 \left( \frac{r_2}{r_1 + r_2} \right) \quad (2)$$

$$V_{02} = E_2 \left( \frac{r_1}{r_1 + r_2} \right) \quad (3)$$

$$V_0 = V_{0w} + V_{01} + V_{02} \quad (4)$$

As mentioned,  $V_{0w}$ ,  $V_{01}$  and  $V_{02}$  are voltages from wind power and the two batteries, respectively, which contribute to the output voltage  $V_0$  independently.

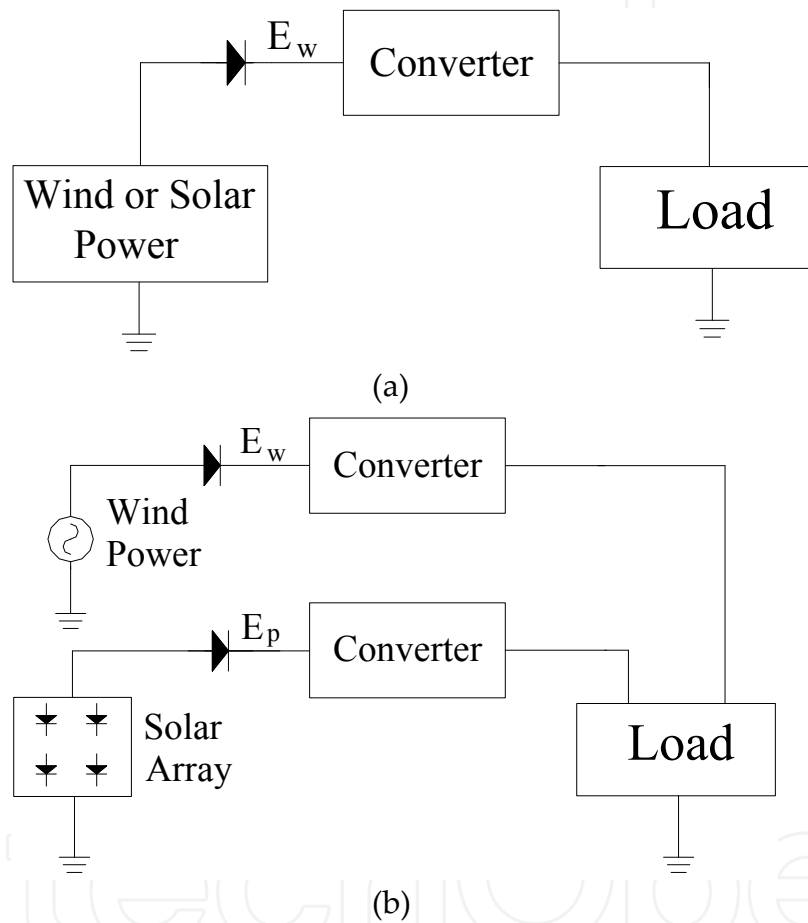


**Figure 1.** (a) Wind or solar power supplies the load through a converter. (b) The wind and solar power use two converters to supply the load at the same time. The voltage and frequency of the converters are adjusted to meet the load requirement.

The following are possible charging situations.

- When  $V_{0w} > V_{01} = V_{02}$ , the charging current from wind power charges simultaneously both batteries  $E_1$  and  $E_2$ .
- When  $V_{0w} > V_{01} > V_{02}$ , the charging currents from both wind power and battery  $E_1$  charge battery  $E_2$ .

- c. When  $V_{ow} > V_{02} > V_{01}$ , similar to case (b), the charging currents from both wind power and battery  $E_2$  charge battery  $E_1$ .
- d. When  $V_{01} > V_{ow} > V_{02}$ , wind power has no effect on the circuit, only battery  $E_1$  charges battery  $E_2$ .
- e. When  $V_{02} > V_{ow} > V_{01}$ , similar to case (d), wind power has no effect on the circuit, only  $E_2$  charges battery  $E_1$ .

As seen in above analysis, it is only in case (a) that wind power can charge both batteries at the same time. However, in case (b), when battery  $E_1$  also charges battery  $E_2$ , the voltage drop of  $I_1 r_1$  and  $I_2 r_2$  cause increase in  $V_{02}$  and decrease in  $V_{01}$  respectively. Finally, when  $V_{01} = V_{02}$ , the charging condition returns to case (a). Case (c) is similar to case (b), so it exhibits self-regulating behavior during the charging process. Cases (d) and (e) are not normal charging conditions.

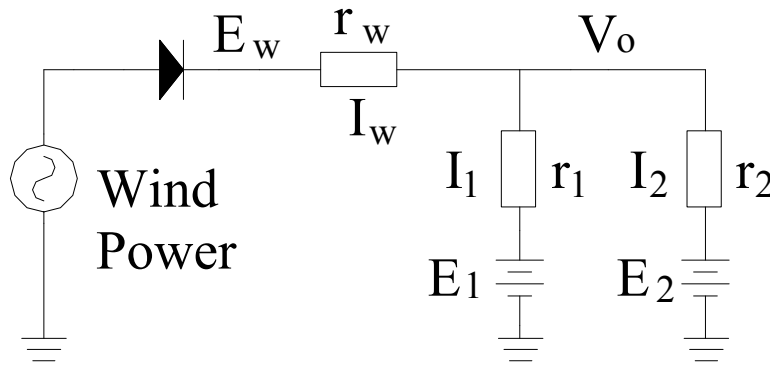


**Figure 2.** Wind power charges both batteries. During the charging process, the increase in charging current  $I_1$  leads to increase in internal voltage drop  $I_1 r_1$ , which raises  $V_o$ , and in turn increases  $I_2$ . Therefore, this charging configuration comprises a self-regulation mechanism.

Figure 3(a) shows a hybrid wind and PV power generating system.  $E_w$ ,  $E_p$ ,  $E_b$ ,  $r_w$ ,  $r_p$  and  $r_b$  are factors that determine the charging current. Similar to the above conventional charging conditions, the output voltage  $V_o$  is made up of  $V_{ow}$ ,  $V_{op}$  and  $V_{ob}$  from the wind generator, solar panel and battery, respectively. The related equations are listed below.

$$V_{ow} = E_w \left( \frac{r_b}{r_w + r_b} \right) \quad (5)$$

$$V_{op} = E_p \left( \frac{r_b}{r_p + r_b} \right) \quad (6)$$

$$V_o = E_b + V_{ow} + V_{op} \quad (7)$$

Possible charging conditions are as follows:

- a. When  $V_{ow} > V_{op} > E_b$ , both wind and solar energies charge the battery.
- b. When  $V_{op} > V_{ow} > E_b$ , both wind and solar energies charge the battery.
- c. When  $V_{ow} > V_{op}$ , only wind energy charges the battery.
- d. When  $V_{op} > V_{ow}$ , only solar energy charges the battery.

From the above analysis, in cases (a) and (b), there are two energy sources charging a battery at the same time. However, in case (a), the larger current  $I_w$  from wind energy may result in a larger internal voltage drop  $I_b r_b$  of the battery. Therefore, when  $V_{ow} > V_{op}$ , the charging condition becomes case (c), and solar energy cannot be utilized to charge the battery. Case (b) shows the same behavior. Contrary to the conventional charging system, the hybrid charging system exhibits a competition effect, meaning that only the larger power source can dominate the charging system.

Figure 3(b) shows the I-V curves of the charging system. Because the source resistance of the wind generator is much smaller than that of the solar panel, the wind I-V curve reduces slowly with increase in charging current. The source resistance of the battery is also much smaller than that of the wind generator. Therefore, the terminal voltage of the battery  $V_o$  increases only slightly with increase in charging current. When the solar I-V curve drops to P, which is equal to the terminal voltage of the battery, the solar energy stops charging the battery.

Figure 3(c) shows the V-T curves of the charging system. Before time  $T_o$ , the battery is in under-charge condition, both power sources behave as the current sources with their ratio of output currents proportional to that of generated power levels. For time  $T_o$  to  $T_t$ , the source resistance of the solar panel lowers gradually the solar charging current and the battery terminal voltage  $V_o$  increases slowly. Finally, at time  $T_t$ , only wind power can charge the battery.

To improve the performance of the hybrid power generating system shown above, a switch control is employed. It is connected to the battery circuit as shown in Fig. 4. In this operation mode, both wind and solar energy can be utilized, although only one energy source can charge the battery at any time. Owing to the different characteristics of wind and solar energy, as shown in Eq. (10), we can adjust the charging duty cycle ratio  $k$  of the two energy sources to obtain maximum energy in the battery. The equations are listed below.

$$V_{ow} = E_b + E_w \left( \frac{r_b}{r_b + r_w} \right) \quad (8)$$

$$V_{op} = E_b + E_p \left( \frac{r_b}{r_b + r_p} \right) \quad (9)$$

$$W = kW_w + (1 - k)W_p \quad (10)$$

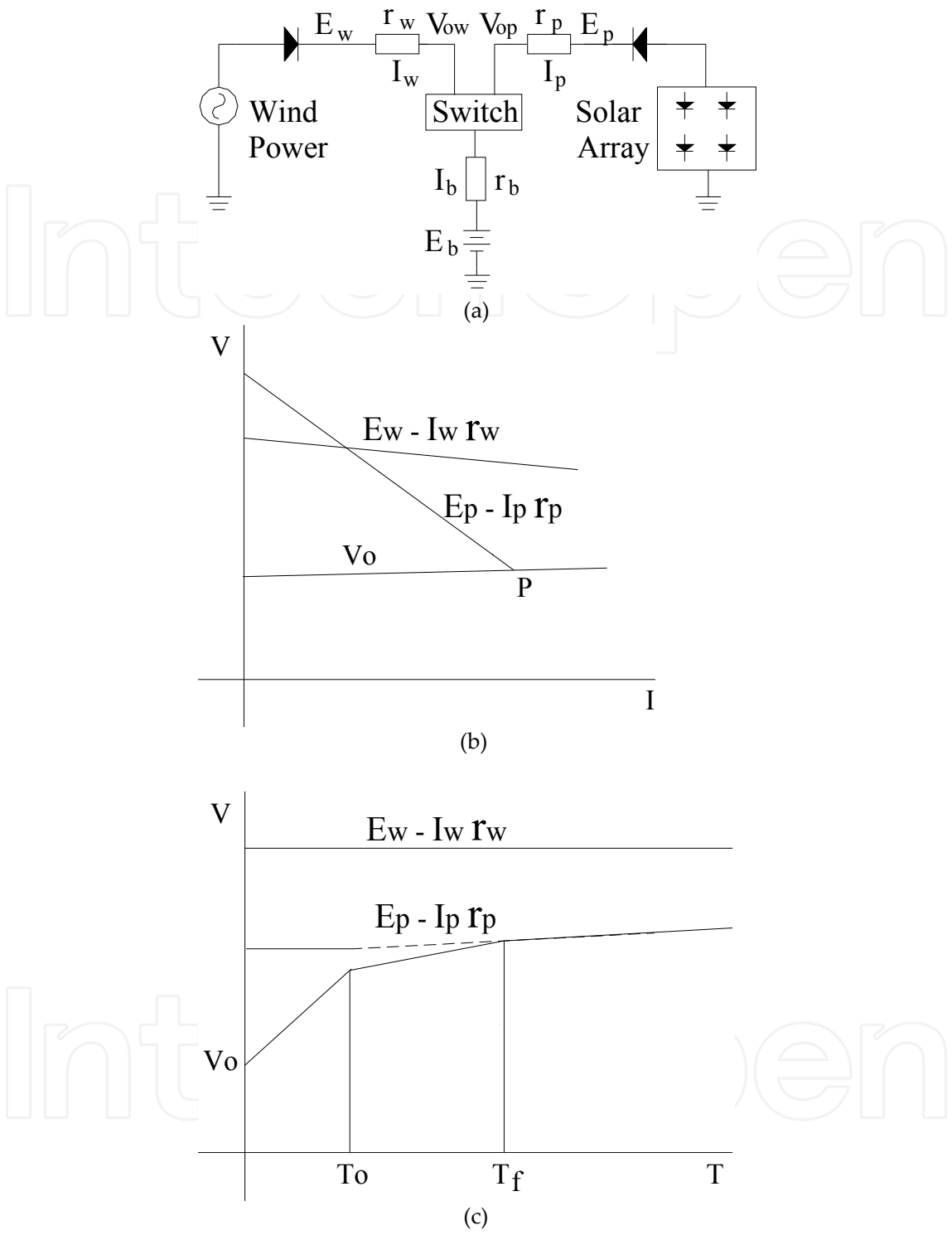


**Figure 3.** (a) Small hybrid wind and PV energy charging system. Two power sources charge a battery. Owing to the internal voltage drop caused by impedance of wind, solar and battery power source, only one power source can contribute to the charging process. (b) I-V characteristics of the charging system. When the solar I-V curve drops to point P, solar power cannot charge the battery. (c) Simplified charging curve of the system. Two current sources charge the battery before time  $T_o$ . Then, charging speed reduces because of increase in resistance of the solar power circuit. After time  $T_f$ , only wind power charges the battery.

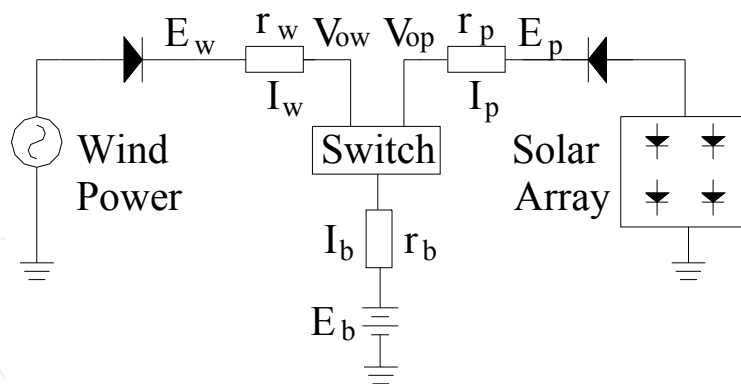


**Figure 4.** Switch-controlled wind and PV energy charging system. The wind and solar power charge a battery alternately. Both power sources can charge the same battery at different times. During solar energy charging, mechanical energy generated by inertia of the wind turbine will be stored and employed to charge the battery during wind energy charging. On the other hand, solar energy cannot be stored but will be lost during wind energy charging. In view of this, we can adjust the wind power charging duration to obtain the maximum energy.

To overcome the drawbacks of the hybrid wind and PV charging system shown above, a microprocessor-controlled power generating system, as shown in Fig.5, is proposed. The different charging modes, which vary with the weather conditions to obtain the maximum energy, are shown in Table 1. With both energy sources, the system operates in the independent charging mode. The wind and solar energy charge batteries  $E_{bw}$  and  $E_{bp}$  respectively. If there is only one energy source, the system runs in the hybrid charging mode. Either energy source can charge batteries  $E_{bw}$  and  $E_{bp}$  simultaneously. Owing to the instability of wind energy, if both energy sources co-exist, wind energy exceeds the threshold value, the charging system runs in the wind-enhanced mode. In this case, not only can both energy sources be employed to improve the reliability of power system, the fluctuations in the small wind power generating system can also be reduced.

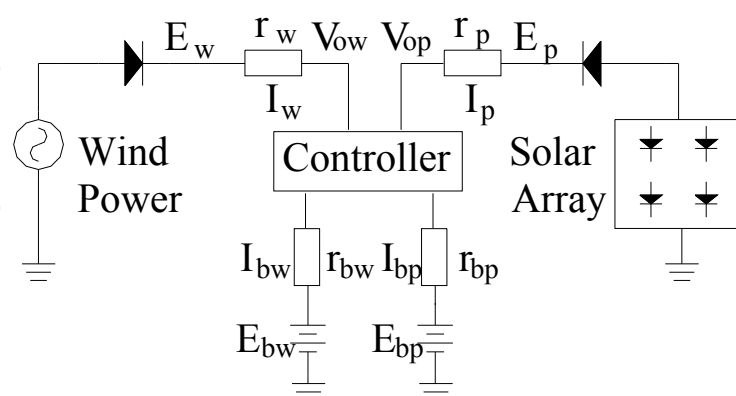


**Figure 5.** Microprocessor-controlled wind and PV energy charging system. Both power sources charge the two batteries. According to the wind and solar energy conditions, the controller regulates the charging conditions for  $E_{bw}$  and  $E_{bp}$ . There is no power loss in this charging system. When there is only one power source, it can charge both batteries. With both power sources and high wind energy, the excess wind energy charges battery  $E_{bp}$ . The controller improves greatly the reliability of this charging system.



Energy Source	Ebw	Ebp
Solar Energy	▲	▲
Wind Energy	▲	▲
Solar and Wind Energy (low wind speed)	●	●
Solar and Wind Energy (high wind speed)	▲	▲
● : Independent Charging    ▲ : Hybrid Charging		
Ebp : Solar Battery                      Ebw : Wind Battery		

**Table 1.** Microprocessor – controlled charging modes, Under independent charging condition, the solar energy and wind energy charges respectively the corresponding battery. Under hybrid charging condition, both energy sources charge the two batteries simultaneously.

3. Results and discussion

3.1. Source resistance measurements

To measure battery source resistance, as shown in Fig. 6(a), a 12-V/75-AH battery supplied the load through a switch. We adjusted the load resistance  $R_L$  to change the battery discharging current  $I_b$ . From the voltage difference  $E_b - V_o$  and  $I_b$ , the source resistance  $r_b$  can be determined. Because the solar energy is much smaller than the battery energy and the solar cell internal resistance  $r_p$  is much larger than the battery source resistance  $r_b$ , as shown in Fig. 6(b), the output terminal of the solar panel is directly grounded to measure the solar charging current  $I_p$ . A 75-W solar cell panel was used in the experiment performed outdoors. From the solar voltage  $E_p$  and the current  $I_p$ , the solar internal resistance can be determined.

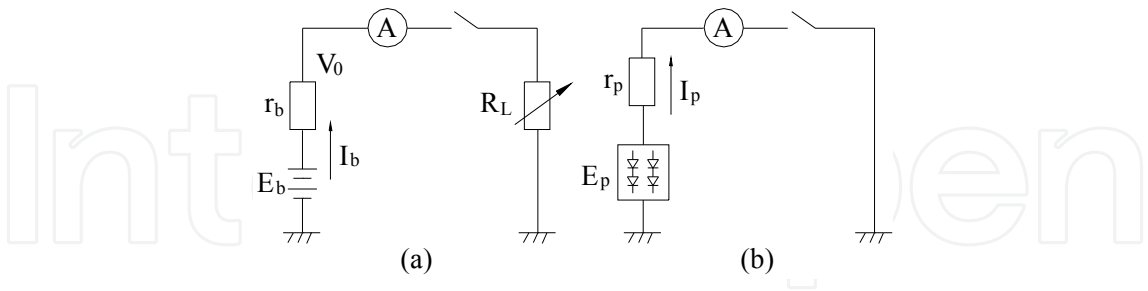


**Figure 6.** (a) Circuit for measuring battery source resistance. Because much energy is stored in the battery  $E_b$  and the battery source resistance  $r_b$  is small,  $R_L$  is employed to limit the discharging current  $I_b$ . (b) Circuit for measuring solar cell internal resistance. Solar current  $I_p$  is varied by adjusting the orientation of the solar cell panel relative to the sun.

As shown in Fig. 7(a), the source resistance of battery decreases with increasing discharge current. The battery source resistance is about 0.02-0.12  $\Omega$  for discharge current 1-13 A. The power loss of the source resistance results in temperature rise of the battery. Hence, chemical reaction proceeds more easily with increasing charging current and the resistance to battery charging is reduced.

The source resistance of solar cell panel, as shown in Fig. 7(b), also decreases with increasing short-circuit current. However, the source resistance of the solar cell panel is much larger than that of battery. Even though the area of the solar cell panel is large, the thickness of the solar cell structure is too small to increase the efficiency of optical absorption. Conventionally, the thickness of the solar cell active layer is in the micrometer range. Moreover, the resistivity of solar cell is large, which results in high source resistance.

The stator of PMG has 36 slots wound with 40 turns of 0.8- $\Phi$  copper wires. The source resistance (one phase) of PMG is found to be 0.5  $\Omega$ . It is much smaller than the source resistance of the solar cell panel (about 6-18  $\Omega$ ). In general, the difference in voltage between wind energy source  $E_w$  and solar energy source  $E_p$  is not large. According to Eqs. (5) and (6), when the wind turbine is in operation, the wind output  $V_{ow}$  is much larger than the solar output  $V_{op}$ . Therefore, the wind turbine dominates the battery charging behavior.

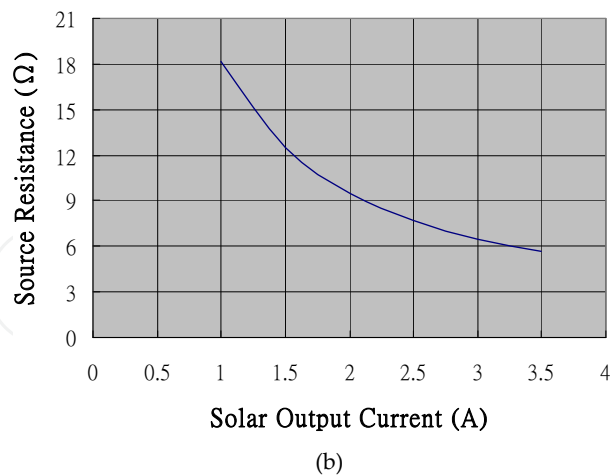
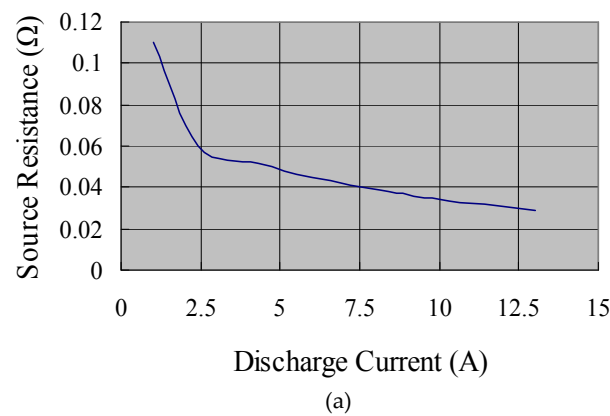


**Figure 7.** Under conventional wind speed, the source impedance of the PMG comes from the resistance of copper winding of the stator. Copper is a good conductor. Therefore, there is only a small variation in resistance when the generator current increases. In (a), the battery stores the chemical energy. Under loaded condition, thermal effect increases with the current in the battery, which speeds up the chemical reaction. Hence, the source resistance of the battery decreases with the current. However, the solar cell is made up of semiconductors. In addition to the high resistance of semiconductors, there is also a large variation in resistance of the solar cell when the current increases, as shown in (b).

### 3.2. Conventional hybrid wind and PV power generating system

In this study, a 250-W permanent magnet alternator driven by wind turbine and a 12-V/75-W solar cell panel were used as the wind and solar energy source, respectively. Both energy sources were output to 12-V/75-AH lead batteries, which were kept in under-charged condition before test. In the experiment, a 100-MHz scope was employed to measure the charging current and battery voltage. A current probe set at 100 mV/A was utilized to sense the charging current. The alternator outputs were converted into DC output by a rectifier module to charge the batteries. As shown in Fig. 8, there was a large variation in current and voltage because of the unstable wind speed. The fluctuations in amplitude of the charging current were attributed to the conventional AC-DC rectification effect. Increase in wind speed also led to increase in charging current. The variation in battery voltage as a result of internal impedance is above 1V.

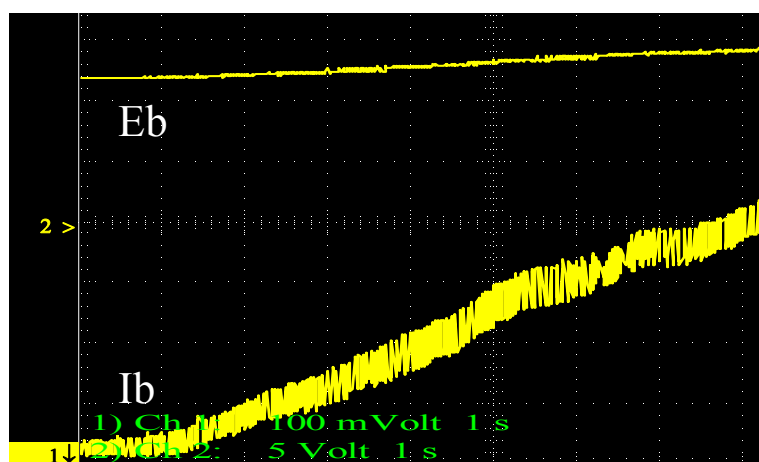
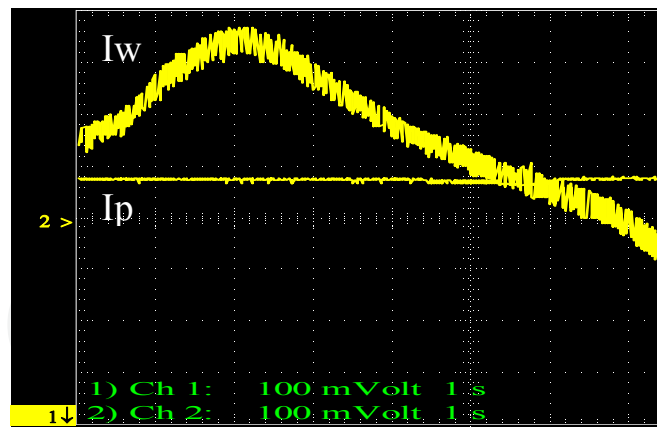
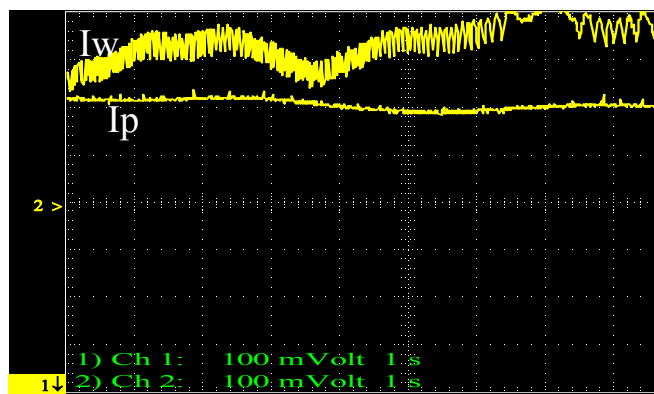


**Figure 8.** Charging current (Ch1: A/div) and battery voltage (Ch2: 5 V/div) of wind power. Owing to the source resistance of the battery, the internal voltage drop increases with the charging current  $I_b$ . This leads to the increase in the battery voltage  $E_b$ .

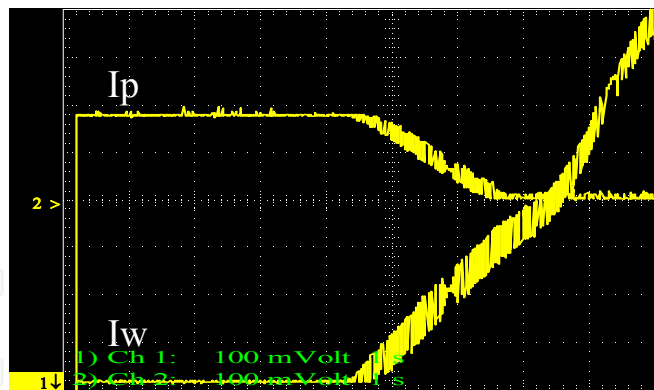
A battery was charged by wind and solar energy sources using the conventional wind and PV charging system, as shown in Fig. 3. In the first 30 minutes, the battery remained in an under-charged condition. As shown in Fig. 9(a), the stable 0.8-A PV charging current is not affected by the large variation in wind charging current. After 1 hour, as seen in Fig. 9(b), the charging curve of solar energy shows an opposite trend as that of wind power. The solar charging current decreases as the wind charging current increases. After 2 hours, as shown in Fig. 9(c), either solar energy or wind power dominates the charging behavior. When the wind charging current exceeds 3 A, the solar energy source does not output any power. Therefore, the system cannot get both wind and solar energy at the same time.



(a)



(b)



(c)

**Figure 9.** Both wind and solar sources charge a single battery. Ch1: wind charging current (A/div), Ch2: solar charging current (A/div). (a) During the first 30 minutes, despite large variations in the wind charging current  $I_w$ , both energy sources charge the battery simultaneously, indicating that the open-circuit battery voltage  $E_b$  is small. (b) After 1-hour charging, competitive behavior occurs. When the wind charging current  $I_w$  exceeds 6.5A, the solar charging current  $I_p$  decreases. The large wind charging current increases the internal voltage drop of the battery, which leads to decrease in solar charging current. (c) After 2-hour charging, a wind charging current of only 0.5 A can reduce the solar charging current from 1.8 A. This points out that the battery voltage builds up gradually and the small internal voltage drop is enough to exclude the solar charging current. Therefore, the small source impedance of the wind generator dominates the charging operation. A wind charging current of only 3 A can stop the solar charging current.

### 3.3. Switch- control hybrid wind and PV power generating system

In order to acquire both wind and solar energy at the same time, the system is configured as in Fig. 4. As seen in Fig. 10(a)-(c), the wind to solar charging duty cycle ratio is changed to examine the charging behavior at three wind speeds. Owing to fluctuations in wind speed at 3 m/s, the system sometimes stops outputting the wind charging current, as seen in Fig. 10(a), while the charging of battery by solar energy remains very stable. When wind speed increases to 4 m/s, as shown in Fig. 10(b), the wind charging current continues to charge the battery during its duty cycle, but the current decreases during charging. When the solar charging duration is increased to 3.2 seconds, the wind charging current drops to 2 A, as seen in Fig. 10(c) prior to solar charging. Upon completion of solar charging, i.e. after 3.2 seconds, the wind charging current increases to 4 A and falls gradually back to 2 A. This phenomenon can be explained as follows. During solar energy charging, the wind turbine is in a no-load condition. Wind energy is thus converted into mechanical energy, which speeds up the alternator. In other words, owing to the inertial momentum, the wind turbine can store mechanical energy, and solar energy is not best utilized or lost during wind charging. Therefore, the charging duty cycle ratio between wind and solar energy can be adjusted to obtain the maximum energy source.

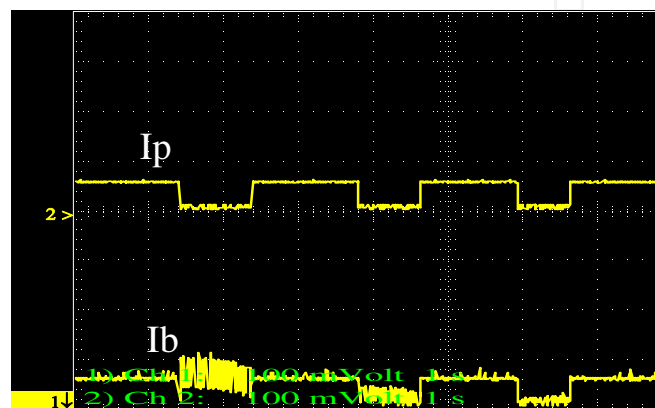
### 3.4. Microprocessor- controlled hybrid wind and PV power generating system

In the above two cases, there is always some energy loss during the power generating system operation. To obtain both wind and solar energy at the same time, a microprocessor and two batteries as shown in Fig. 5 are employed to control the charging operation from both energy sources. Figure 11 displays the circuit in detail, in which controller IC1 and comparator IC2 control the system operation. Depending on the weather condition, wind energy can charge the wind battery  $E_{bw}$  directly or the solar battery  $E_{bp}$  indirectly through  $Q_{ws}$ . Both wind and solar energy are sensed by two comparators of IC2. One senses the sunlight to control the load while the other monitors the charging condition of the wind battery. If there has been no wind or sun for some days and both wind and solar energies remain insufficient, the two batteries will be in under-charged condition and utility power supply will be used instead. In view of large variations in wind energy, a current transformer CT is employed to detect the charging current of the wind battery. If the charging current exceeds the specification of the battery,  $Q_w$  runs in PWM mode to protect the battery. All functions are controlled by the software of controller IC1.

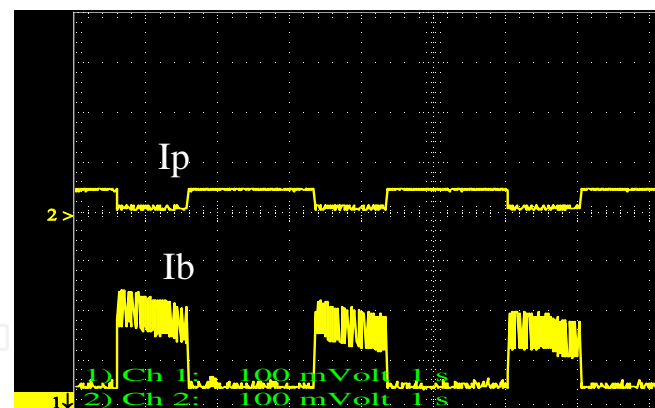
As shown in Fig. 12, when wind speed is low, about 3 m/s, the system runs in the independent charging mode and the solar battery charging current remains constant at 2A, although there are slight variations in the charging current of the wind battery.

If there is only wind power, as shown in Fig. 14(a), the system runs in the wind- hybrid charging mode, so the unstable wind charging current charges both wind and solar batteries. When the charging current is less than 2 A, as shown in Fig. 14(b), the system remains in the wind- hybrid charging mode and only the wind battery is being charged.

When there is solar energy and a high wind speed at the same time, as shown in Fig. 15, the system runs in the wind-enhanced charging mode. In order to benefit from both energy sources and reduce fluctuations from the wind source, the system runs in the wind-enhanced charging mode when the wind charging current is above 3A. The wind charging current charges the solar battery in addition to the original wind battery, leading to variations in the solar charging current. When the wind charging current is below 3A, the system runs in the independent charging mode. That is, the stable solar charging current of 2A and the fluctuating wind charging current charge the solar battery and the wind battery, respectively.



(a)



(b)

**Figure 10.** Switch-controlled wind and solar sources charge a battery. Ch1: battery charging current (A/div), Ch2: solar charging current (a),(b), wind charging current (c) (A/div). (a) Wind speed is 3 m/s, but it is unstable. The charging duty cycle ratio between solar and wind power is 2:1. In the absence of wind power, only the solar charging current (0.6 A) charges the battery. In the presence of wind power, the wind charging current gradually decays. Because the wind charging duration is only 0.8 second, steady state cannot be attained. (b) Wind speed is increased to about 4 m/s and solar charging current is decreased to 0.4 A. Wind energy exceeds solar energy. (c) Wind speed is increased to 5 m/s. The charging duty cycle ratio between solar and wind power is changed to 1:2. Moreover, the solar charging duration is extended from 1.8 to 3.2 seconds. In this situation, mechanical energy accumulated by inertia of the wind turbine during solar charging can also be utilized during wind charging. Hence, this configuration can ensure full utilization of wind energy with no loss at all.

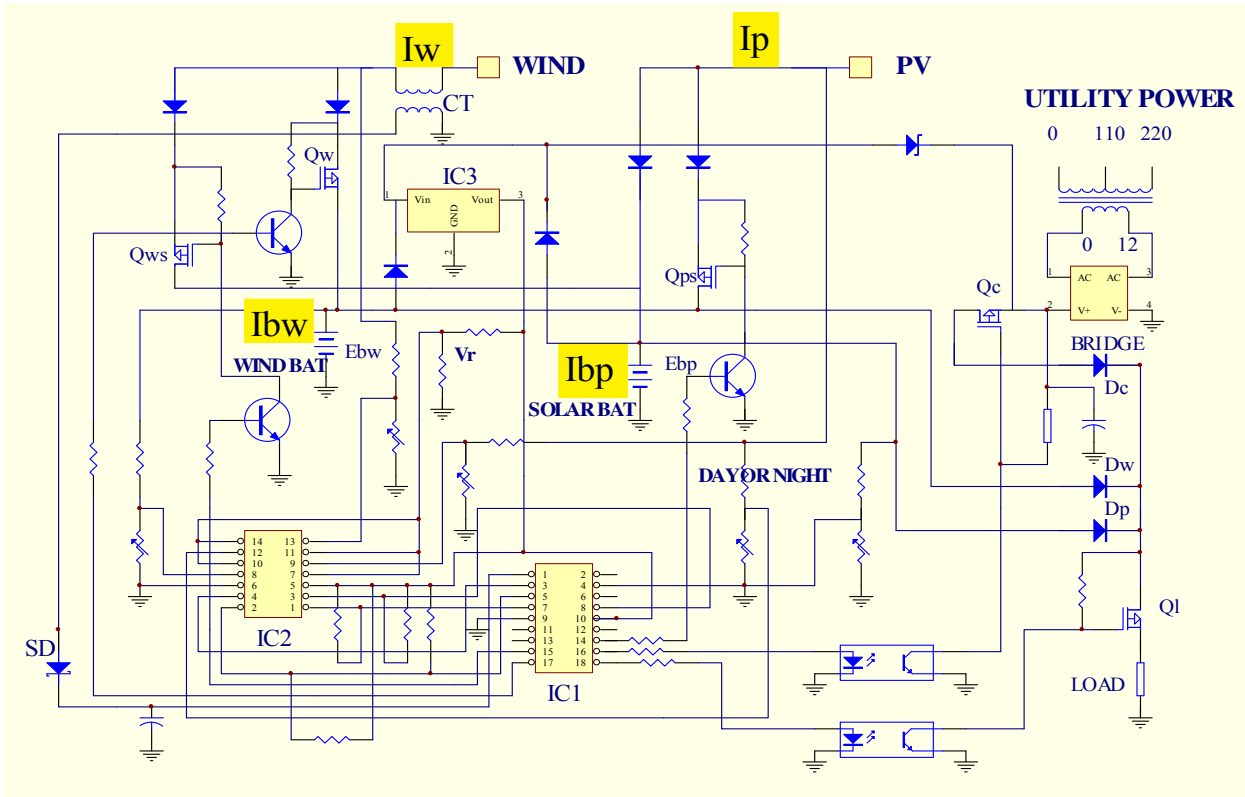


**Figure 11.** Microprocessor-controlled hybrid wind and solar charging circuit. Microprocessor IC1 and Comparator IC2 controls the wind charging current  $I_w$  and the solar charging current  $I_p$  that fuel the wind ( $E_{bw}$ ) and solar ( $E_{bp}$ ) battery. According to the weather condition, the wind and solar charging currents may charge either the wind or solar battery. Current transformer CT senses the wind charging current to prevent damage to the battery by excess charging current. If the energy of the batteries cannot meet the power required, utility power supply is used instead.

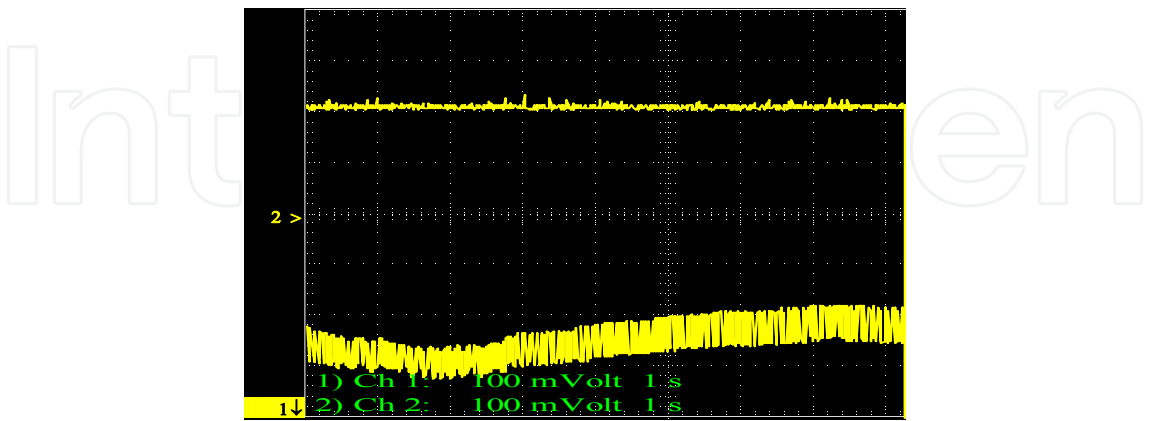


**Figure 12.** Both solar and wind power co-exist. The controller operates in the independent charging mode. The wind charging current charges the wind battery (Ch1: A/div) while the solar charging current charges the solar battery (Ch2: A/div).

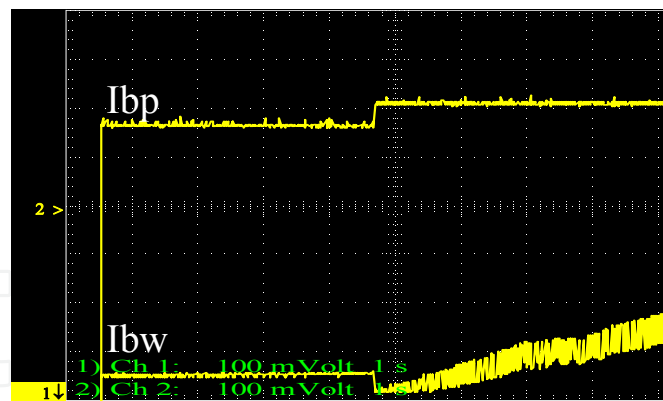
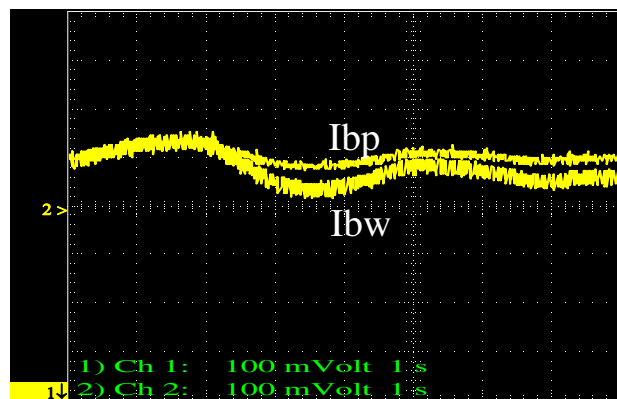
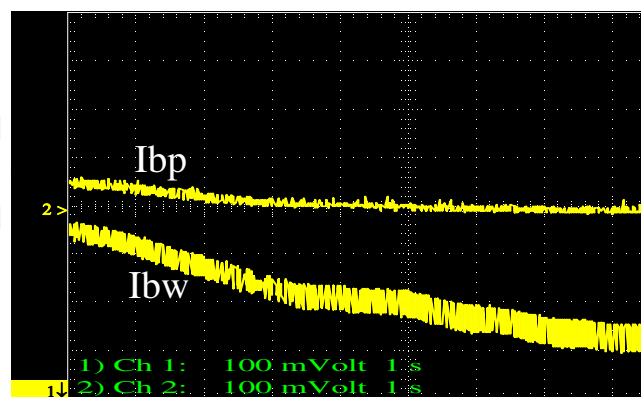


**Figure 13.** The charging system operates in two stages. In Stage 1, only solar energy exists. The solar charging current not only charges the solar battery but also the wind battery. In Stage 2, when wind power also exists, the wind charging current charges the wind battery. Part of the solar charging current is switched back to the solar battery. Ch1, Ch2: A/div.



(a)



(b)

**Figure 14.** The charging system operates when there is only wind power. (a) When wind speed exceeds 5 m/s, the wind charging current charges both wind and solar batteries. (b) When wind speed drops gradually below 3 m/s, the wind charging current in the solar battery decreases to zero. Ch1, Ch2: A/div



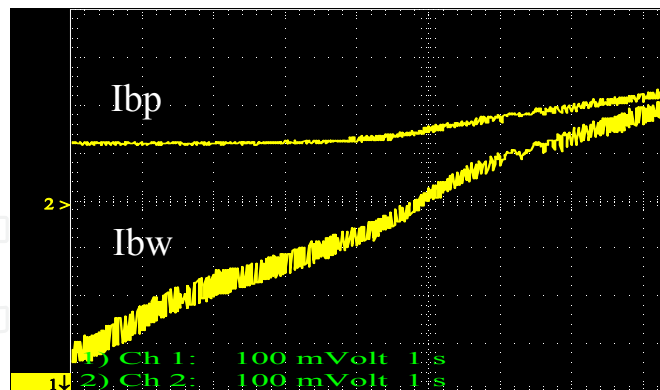


**Figure 15.** Both wind and solar power sources co-exist, but wind speed sometimes exceeds 8 m/s. The charging system operates in two stages. In Stage 1, when wind speed is below 5 m/s, same as that in Fig. 12, the solar and wind charging currents charge the solar and wind battery, respectively. In Stage 2, when wind speed is increased, the wind charging current not only charges the wind battery, but also the solar battery. That is, there are two currents charging the solar battery. Ch1, Ch2: A/div

## 4. Conclusion

In this study, theoretical investigations are performed to examine the effect of source impedance on a small hybrid wind and PV power system. Because of voltage drop in power sources, both energy sources cannot charge a battery simultaneously after initial charging. This study proposed using a switch circuit to increase the utilization of both energy sources. There is only slight solar energy loss when wind power is in operation. To increase energy efficiency by gaining both wind and solar energy, a microprocessor-based hybrid charging system is proposed. Results show that besides increasing the reliability of the power system, the fluctuations in wind energy source are also reduced.

## Author details

Mu-Kuen Chen and Chao-Yuan Cheng

Department of Electrical Engineering, St. John's University, Taiwan

## References

- [1] Salameh, Z. M., Casacca, M. A. and Lynch, W. A. "A mathematical model for lead-acid batteries," *IEEE Trans. On Energy Conversion*, vol.7, no.1, pp 93-98, Mar. 1992.

- [2] H. G. Zimmerman and R. G. Peterson, "An electrochemical cell equivalent circuit for storage battery/power system calculations by digital computer", Proceedings 13<sup>th</sup> Intersociety Energy Conversion Engineering Conference, pp. 33-38, 1978.
- [3] Harrington, S. and Dunlop, J. "Battery charge controller characteristics in photovoltaic systems," *IEEE AES Magazine*, pp 15-21, Aug. 1992
- [4] Masoum, M. A. S., Badejani, S. M. M. and Fuchs, E. F., "Microprocessor-controlled new class of optimal battery chargers for photovoltaic applications," *IEEE Trans. On Energy Conversion*, vol.19, no.3, pp 599-606, Sep. 2004.
- [5] Casacca, M. A., Capobianco, M. R. and Salameh, Z. M. "Lead acid battery storage configurations for improved available capacity," *IEEE Trans. On Energy Conversion*, vol.11, no.3, pp 139-145, Mar. 1996.
- [6] Koutroulis E. and Kalaitzakis K., "Novel battery charging regulation system for photovoltaic applications," *IEE Proc. Electr. Power Appl.* vol.151, no.2, pp 191-197, March 2004
- [7] Jiang Z. and Dougal, R. A. "Control strategies for active power sharing in a fuel-cell-powered battery-charging station," *IEEE Trans. On Industry Applications*, vol. 40, no. 3, pp 917-924, May/Jun, 2004
- [8] Borowy, B. S. and Salameh, Z. M., "Optimum photovoltaic array size for a hybrid wind/PV system," *IEEE Trans. On Energy Conversion*, vol.9, no.3, pp 482-488, Sep. 1994.
- [9] Chedid, R. and Rahman, S., "Unit sizing and control of hybrid wind-solar power systems," *IEEE Trans. On Energy Conversion*, vol.2, no.1, pp 79-85, Mar. 1997.

IntechOpen

